

Supporting information

**A superior catalyst with dual redox cycles for the selective reduction  
of NO<sub>x</sub> by ammonia**

**Zhiming Liu, \*<sup>a</sup> Yang Yi,<sup>a</sup> Junhua Li,<sup>\*b</sup> Seong Ihl Woo,<sup>c</sup> Baoyi Wang,<sup>d</sup> Xingzhong Cao,<sup>d</sup>  
and Zhuoxin Li<sup>d</sup>**

<sup>a</sup> State Key Laboratory of Chemical Resource Engineering, Beijing University of Chemical  
Technology, Beijing 100029, China

<sup>b</sup> School of Environment, Tsinghua University, Beijing 100084, China

<sup>c</sup> Department of Chemical and Biomolecular Engineering, Korea Advanced Institute of Science  
and Technology, Daejeon 305-701, Republic of Korea

<sup>d</sup> Key laboratory of Nuclear Analytical Techniques, Institute of High Energy Physics, Chinese  
Academy of Sciences, Beijing 100049, China.

---

\* Corresponding author. Tel: +86-10-64427356  
E-mail: [liuzm@mail.buct.edu.cn](mailto:liuzm@mail.buct.edu.cn) (Z. Liu); [lijunhua@tsinghua.edu.cn](mailto:lijunhua@tsinghua.edu.cn) (J. Li).

## 1. Catalyst preparation and catalytic tests

The Cu-Ce-Ti catalysts with different ratio of Cu/Ce/Ti were prepared by the hydrothermal method. Appropriate amounts of  $\text{Cu}(\text{NO}_3)_2 \cdot 3\text{H}_2\text{O}$ ,  $\text{Ce}(\text{NO}_3)_3 \cdot 6\text{H}_2\text{O}$  and  $\text{Ti}(\text{SO}_4)_2$  were dissolved in deionized water at room temperature and stirred for 1 hour, then ammonia solution was added slowly to the above solution under vigorous stirring until pH is ca. 11. After stirring for 2 h, the obtained suspension was transferred to a Teflon-sealed autoclave and aged at 120 °C for 48 h. The obtained precipitate was filtered and washed with deionized water thoroughly. The resulting powder was dried at 120 °C for 12 h and then calcined in air at 500 °C for 6 h. In comparison, Cu-Ti, Ce-Ti and  $\text{TiO}_2$  were also prepared by the same preparation method as described above. The state-of-the art SCR  $\text{V}_2\text{O}_5\text{-WO}_3/\text{TiO}_2$  catalyst with 1 wt.%  $\text{V}_2\text{O}_5$  and 5 wt.%  $\text{WO}_3$  was also prepared by the conventional impregnation method using  $\text{NH}_4\text{VO}_3$ ,  $(\text{NH}_4)_{10}\text{W}_{12}\text{O}_{41}$ ,  $\text{H}_2\text{C}_2\text{O}_4 \cdot 2\text{H}_2\text{O}$  as precursors and  $\text{TiO}_2$  as the support. After impregnation, the sample was then dried at 120 °C for 12 h and calcined at 500 °C for 4h.

The activity measurements were carried out in a fixed-bed quartz reactor using a 0.12 g catalyst of 40-60 meshes. The feed gas mixture contained 500 ppm NO, 500 ppm  $\text{NH}_3$ , 0 or 5%  $\text{H}_2\text{O}$ , 0 or 50 ppm  $\text{SO}_2$ , 5%  $\text{O}_2$  and helium as the balance gas. The total flow rate of the feed gas was  $300 \text{ cm}^3 \text{ min}^{-1}$ , corresponding to a GHSV of 64,000  $\text{h}^{-1}$ . The reaction temperature was increased from 150 °C to 400 °C in steps of 50 °C. The composition of the product gas was analyzed by a chemiluminescence NO/ $\text{NO}_2$  analyzer (Thermal Scientific, model 42i-HL) and gas chromatograph

(Shimadzu GC 2014 equipped with Porapak Q and Molecular sieve 5A columns). A molecular-sieve 5A column was used for the analysis of N<sub>2</sub> and Porapak Q column for that of N<sub>2</sub>O. The activity data were collected when the catalytic reaction practically reached steady-state condition at each temperature.

## 2. Catalyst characterization

X-ray diffraction (XRD) measurements were carried out on a Rigaku D/MAX-RB X-ray Diffractometer with Cu K $\alpha$  radiation. XPS measurements were conducted on an ESCALab220i-XL electron spectrometer from VG Scientific using 300W Mg K $\alpha$  radiation, calibrated internally by carbon deposit C 1s binding energy (BE) at 284.8 eV. A least-square routine of peak fitting was used for the analysis of XPS spectra. Positron annihilation experiments were performed with a fast-slow coincidence ORTEC system with a time resolution of 196 ps full width at half maximum. A  $5 \times 10^5$  Bq source of <sup>22</sup>Na was sandwiched between two identical samples. Temperature-programmed reduction (H<sub>2</sub>-TPR) experiments were conducted on a chemisorption analyzer (Micromeritics, ChemiSorb 2720 TPx) under a 10% H<sub>2</sub> gas flow (50 mL min<sup>-1</sup>) at a rate of 10 °C min<sup>-1</sup> up to 650 °C.

The structure of catalysts was studied by the micro-Raman spectroscopy (Renisaw, InVia) under the 532 nm<sup>-1</sup> excitation laser light. In situ DRIFTS experiments were performed on an FTIR spectrometer (Nicolet Nexus 870) equipped with a smart collector and an MCT detector cooled by liquid nitrogen. Prior to each experiment, the sample was pretreated at 400 °C for 1 h in a flow of helium and then cooled down to 200 °C. The background spectrum was collected in flowing helium and

automatically subtracted from the sample spectrum. The reaction conditions were controlled as follows: 100 mL min<sup>-1</sup> total flow rate, 500 ppm NH<sub>3</sub> or 500 ppm NO + 5 % O<sub>2</sub>, and helium as the balance. All spectra were recorded by accumulating 100 scans with a resolution of 4 cm<sup>-1</sup>.

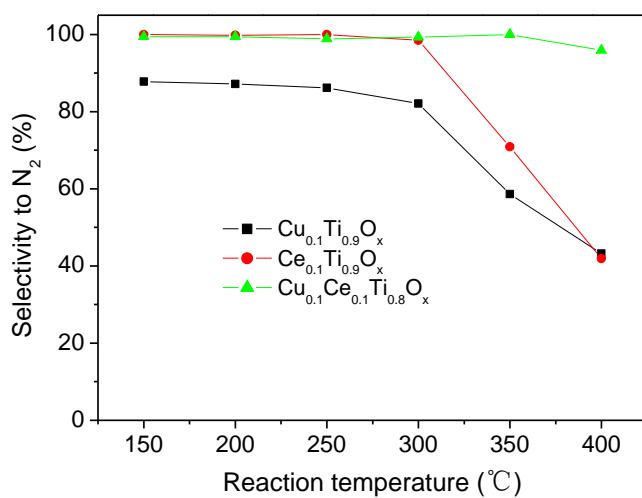


**Fig. S1** N<sub>2</sub> selectivities of Cu<sub>0.1</sub>Ti<sub>0.9</sub>O<sub>x</sub>, Ce<sub>0.1</sub>Ti<sub>0.9</sub>O<sub>x</sub> and Cu<sub>0.1</sub>Ce<sub>0.1</sub>Ti<sub>0.8</sub>O<sub>x</sub> catalysts

(500 ppm NO, 500 ppm NH<sub>3</sub>, 5% O<sub>2</sub>, balance He, GHSV= 64,000 h<sup>-1</sup>)

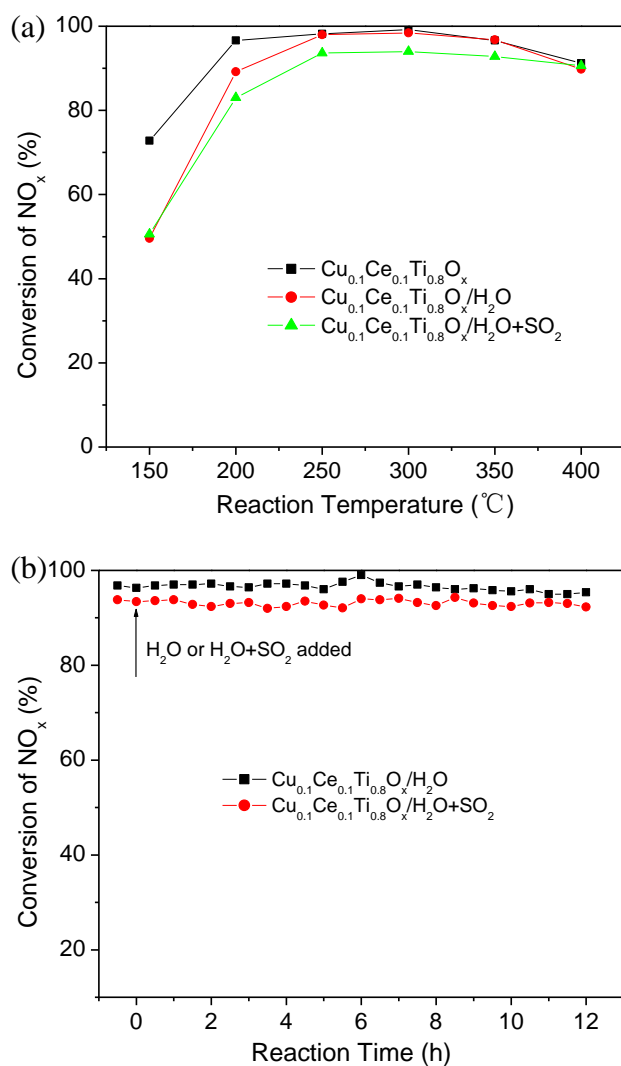


**Fig. S2** NO<sub>x</sub> conversion as a function of temperature (a) and as a function of time at 250 °C (b) over Cu<sub>0.1</sub>Ce<sub>0.1</sub>Ti<sub>0.8</sub>O<sub>x</sub> catalyst in the presence of H<sub>2</sub>O and SO<sub>2</sub> (500 ppm NO, 500 ppm NH<sub>3</sub>, 5% O<sub>2</sub>, 5% H<sub>2</sub>O, 50 ppm SO<sub>2</sub>, balance He, GHSV= 64,000 h<sup>-1</sup>).

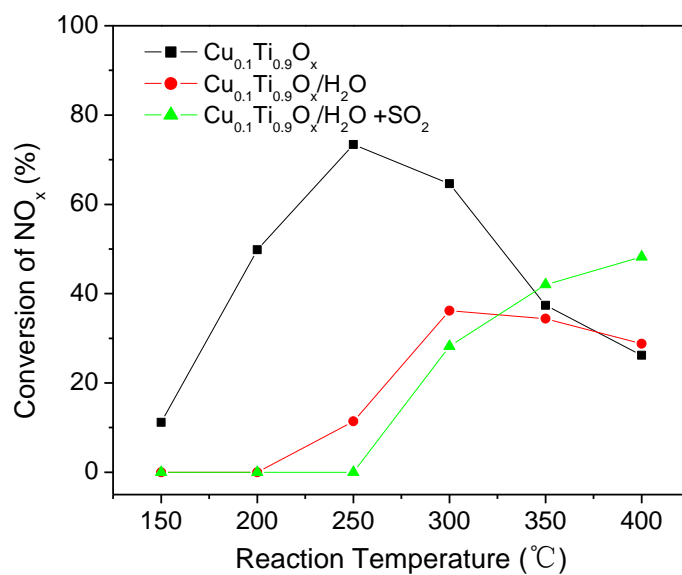


**Fig. S3** The effects of H<sub>2</sub>O and SO<sub>2</sub> on the activity of Cu<sub>0.1</sub>Ti<sub>0.9</sub>O<sub>x</sub> catalysts (500 ppm NO, 500 ppm NH<sub>3</sub>, 5% O<sub>2</sub>, 5% H<sub>2</sub>O, 50 ppm SO<sub>2</sub>, balance He, GHSV=64,000 h<sup>-1</sup>).

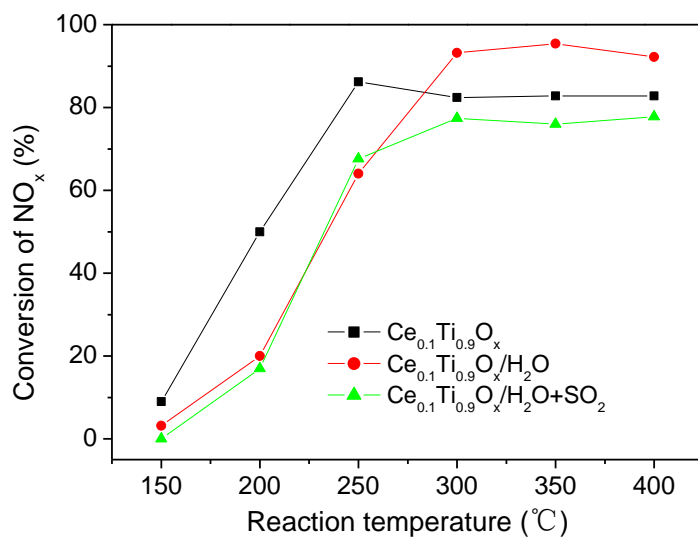


**Fig. S4** The effects of H<sub>2</sub>O and SO<sub>2</sub> on the activity of Ce<sub>0.1</sub>Ti<sub>0.9</sub>O<sub>x</sub> catalysts (500 ppm NO, 500 ppm NH<sub>3</sub>, 5% O<sub>2</sub>, 5% H<sub>2</sub>O, 50 ppm SO<sub>2</sub>, balance He, GHSV=64,000 h<sup>-1</sup>).



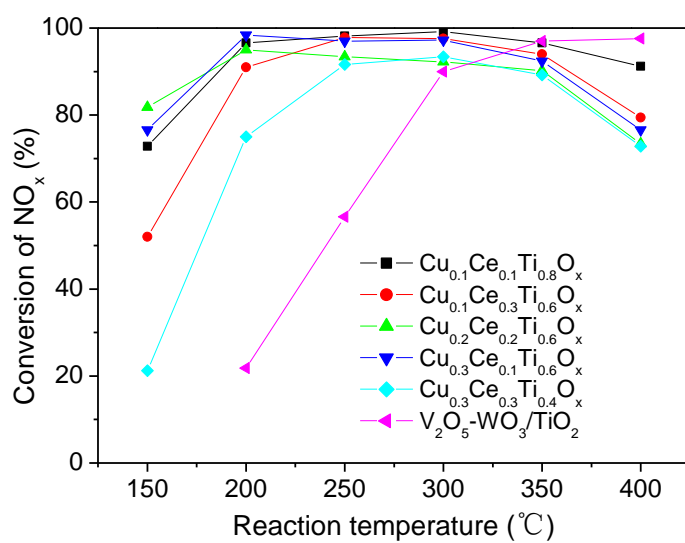


**Fig. S5** Comparison of NH<sub>3</sub>-SCR activity of Cu-Ce-Ti catalysts with that of V<sub>2</sub>O<sub>5</sub>-WO<sub>3</sub>/TiO<sub>2</sub> (500 ppm NO, 500 ppm NH<sub>3</sub>, 5% O<sub>2</sub>, balance He, GHSV=64,000 h<sup>-1</sup>).

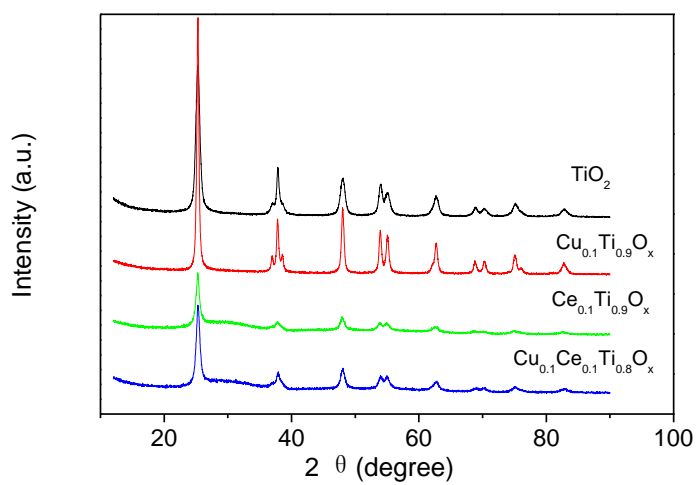


**Fig. S6** XRD patterns of TiO<sub>2</sub>, Cu<sub>0.1</sub>Ti<sub>0.9</sub>O<sub>x</sub>, Ce<sub>0.1</sub>Ti<sub>0.9</sub>O<sub>x</sub> and Cu<sub>0.1</sub>Ce<sub>0.1</sub>Ti<sub>0.8</sub>O<sub>x</sub>.

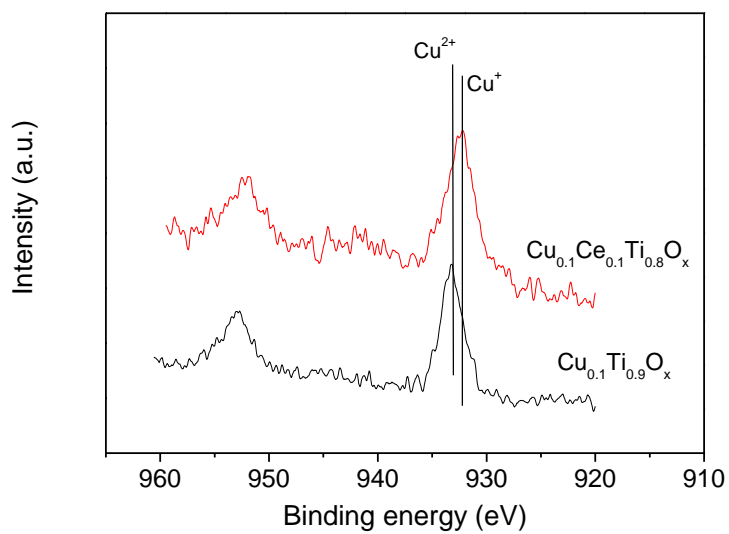


**Fig. S7** Cu 2p XPS spectra of  $\text{Cu}_{0.1}\text{Ti}_{0.9}\text{O}_x$  and  $\text{Cu}_{0.1}\text{Ce}_{0.1}\text{Ti}_{0.8}\text{O}_x$  catalysts.

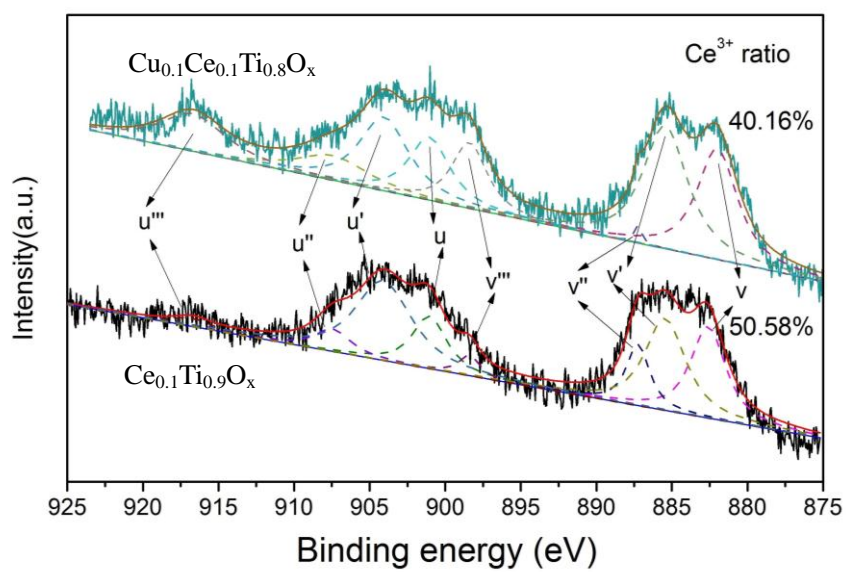


**Fig. S8** Ce 3d XPS spectra of  $\text{Ce}_{0.1}\text{Ti}_{0.9}\text{O}_x$  and  $\text{Cu}_{0.1}\text{Ce}_{0.1}\text{Ti}_{0.8}\text{O}_x$  catalysts.

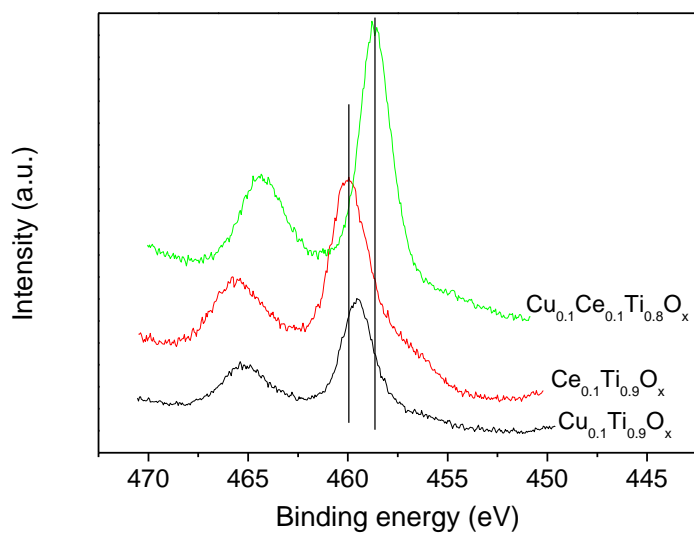


**Fig. S9** Ti 2p XPS spectra of  $\text{Cu}_{0.1}\text{Ti}_{0.9}\text{O}_x$ ,  $\text{Ce}_{0.1}\text{Ti}_{0.9}\text{O}_x$  and  $\text{Cu}_{0.1}\text{Ce}_{0.1}\text{Ti}_{0.8}\text{O}_x$  catalysts.

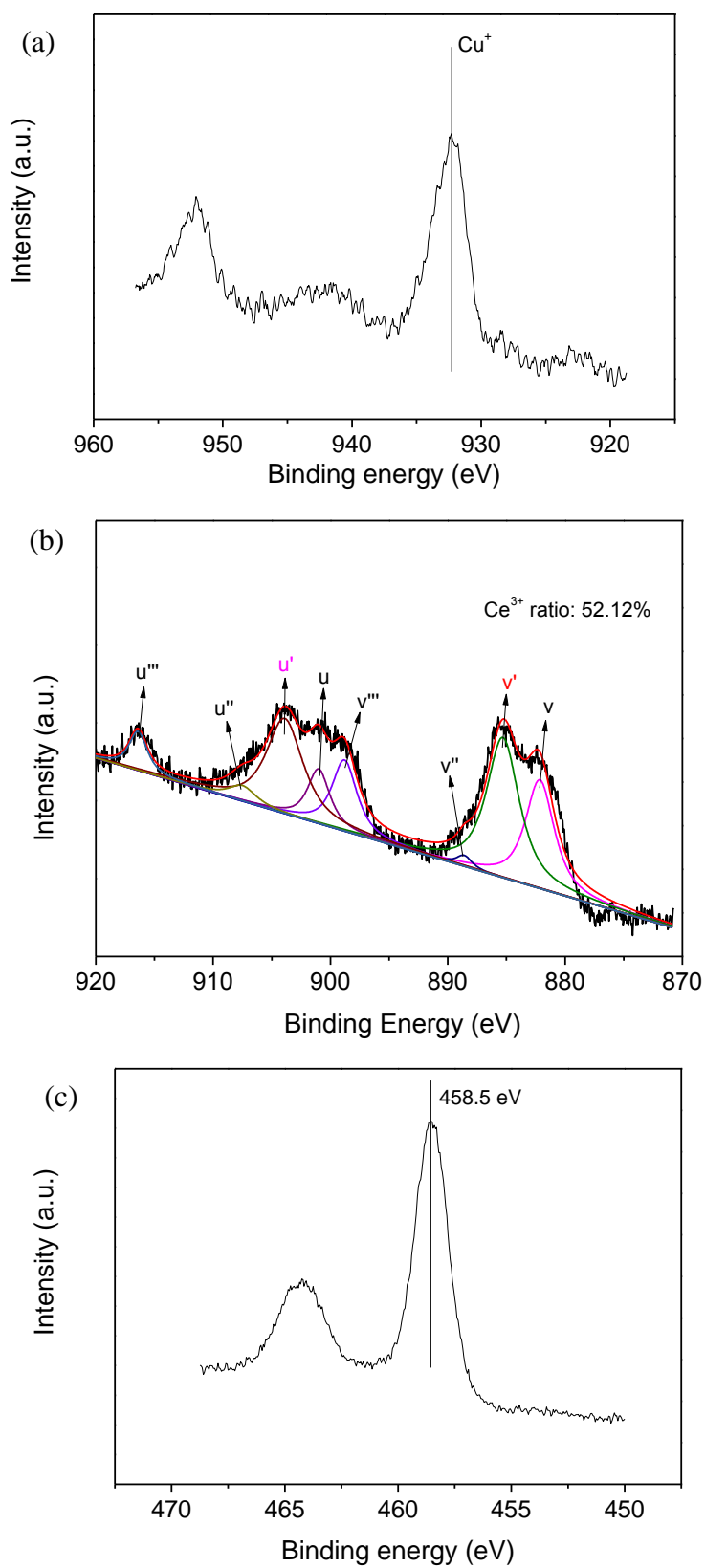


**Fig. S10** Cu 2p(a), Ce3d(b) and Ti2p(c) XPS spectra of the used Cu<sub>0.1</sub>Ce<sub>0.1</sub>Ti<sub>0.8</sub>O<sub>x</sub> catalyst.

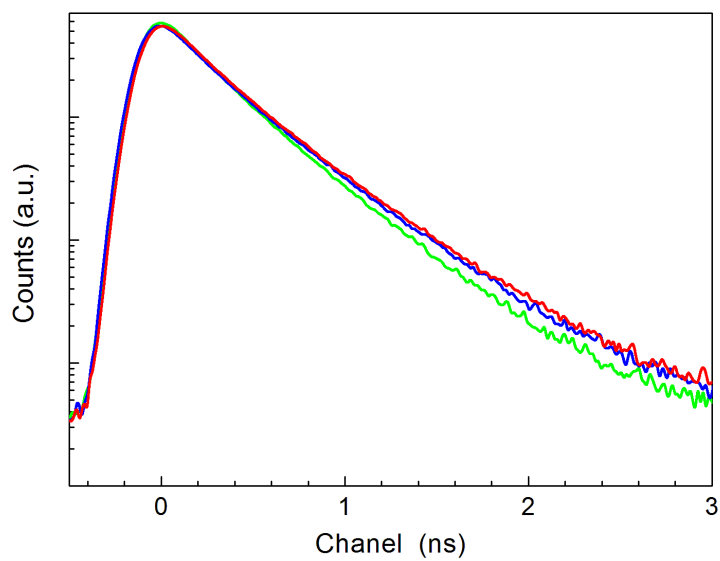


**Fig. S11** The lifetime spectra of  $\text{Cu}_{0.1}\text{Ti}_{0.9}\text{O}_x$  (—),  $\text{Ce}_{0.1}\text{Ti}_{0.9}\text{O}_x$  (—) and  $\text{Cu}_{0.1}\text{Ce}_{0.1}\text{Ti}_{0.8}\text{O}_x$  (—) catalysts.

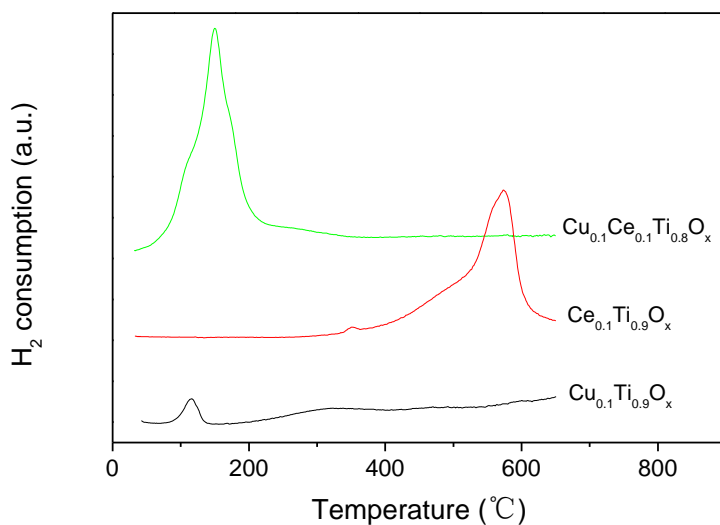


**Fig. S12** H<sub>2</sub>-TPR profiles of Cu<sub>0.1</sub>Ti<sub>0.9</sub>O<sub>x</sub>, Ce<sub>0.1</sub>Ti<sub>0.9</sub>O<sub>x</sub> and Cu<sub>0.1</sub>Ce<sub>0.1</sub>Ti<sub>0.8</sub>O<sub>x</sub> catalysts.

Temperature-programmed reduction (H<sub>2</sub>-TPR) analysis was conducted to investigate the reduction behavior of Cu<sub>0.1</sub>Ti<sub>0.9</sub>O<sub>x</sub>, Ce<sub>0.1</sub>Ti<sub>0.9</sub>O<sub>x</sub> and Cu<sub>0.1</sub>Ce<sub>0.1</sub>Ti<sub>0.8</sub>O<sub>x</sub> catalysts. As illustrated in Fig.S12, Cu<sub>0.1</sub>Ti<sub>0.9</sub>O<sub>x</sub> shows a hydrogen consumption peak at 120 °C, which is attributed to the reduction of CuO particles being in strong interaction with the TiO<sub>2</sub>.<sup>1,2</sup> The reduction peak is significantly lower than that of the bulk and unsupported CuO, which is reduced at about 300 °C.<sup>3</sup> Ce<sub>0.1</sub>Ti<sub>0.9</sub>O<sub>x</sub> exhibited two reduction peaks at around 350 and 570 °C. The former small peak is probably assigned to the reduction of the surface oxygen of ceria and the second reduction peak is due to the reduction of Ce<sup>4+</sup> to Ce<sup>3+</sup>.<sup>1,4</sup> Interestingly, the Cu<sub>0.1</sub>Ce<sub>0.1</sub>Ti<sub>0.8</sub>O<sub>x</sub> catalyst possesses an intense peak centering around 150 °C and the reduction peak starts at lower temperature compared with Cu<sub>0.1</sub>Ti<sub>0.9</sub>O<sub>x</sub> catalyst.



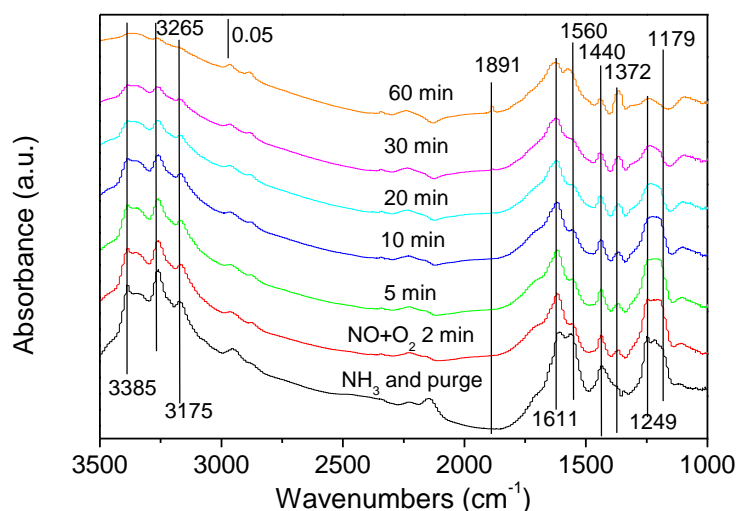


**Fig. S13** In situ DRIFTS of NO+O<sub>2</sub> reacted with pre-adsorbed NH<sub>3</sub> species at 200 °C over Cu<sub>0.1</sub>Ce<sub>0.1</sub>Ti<sub>0.8</sub>O<sub>x</sub> catalyst.

The DRIFT spectra of NO+O<sub>2</sub> adsorption over Cu<sub>0.1</sub>Ti<sub>0.9</sub>O<sub>x</sub>, Ce<sub>0.1</sub>Ti<sub>0.9</sub>O<sub>x</sub> and Cu<sub>0.1</sub>Ce<sub>0.1</sub>Ti<sub>0.8</sub>O<sub>x</sub> catalysts at 200°C was investigated. Several distinct bands at 1891, 1625, 1601, 1585, 1375, 1274, 1235 and 1218 cm<sup>-1</sup> were observed, which were respectively assigned to the gas phase or weakly adsorbed NO (1891 cm<sup>-1</sup>),<sup>5</sup> adsorbed NO<sub>2</sub> (1601, 1625 cm<sup>-1</sup>),<sup>5,6</sup> bidentate nitrate (1585 cm<sup>-1</sup>),<sup>7,8</sup> bridging nitrate (1274, 1235 and 1218 cm<sup>-1</sup>)<sup>7,8</sup> and M-NO<sub>2</sub> nitro compounds (1375 cm<sup>-1</sup>).<sup>10</sup>

In the case of NH<sub>3</sub> adsorption over these three catalysts, the bands at 1611, 1249 and 1179 cm<sup>-1</sup> can be assigned to the coordinated NH<sub>3</sub> on Lewis acid sites,<sup>10, 11</sup> and that at 3385, 3265 and 3175 cm<sup>-1</sup> can be ascribed to the N-H stretching vibration modes of the coordinated NH<sub>3</sub>.<sup>11</sup> The ionic NH<sub>4</sub><sup>+</sup> bound to Brønsted acid sites (1440 cm<sup>-1</sup>)<sup>8</sup> was also observed over Ce<sub>0.1</sub>Ti<sub>0.9</sub>O<sub>x</sub> and Cu<sub>0.1</sub>Ce<sub>0.1</sub>Ti<sub>0.8</sub>O<sub>x</sub> catalysts, with the N-H stretching vibration modes of NH<sub>4</sub><sup>+</sup> (2959 cm<sup>-1</sup>).<sup>12</sup> The peak at 1560 cm<sup>-1</sup> can be

assigned to the scissoring vibration mode of  $\text{NH}_2$  species.<sup>9</sup>

The reactivity of adsorbed  $\text{NH}_3$  species towards  $\text{NO} + \text{O}_2$  was evaluated by the time-dependent changes of the IR spectra at 200 °C and the results are shown in Fig. S13. After the catalyst was exposed to  $\text{NH}_3$  for the 60 min and purged with helium, the adsorbed  $\text{NH}_3$  on Lewis acid sites (3385, 3265, 3175, 1611, 1249 and 1179  $\text{cm}^{-1}$ ),<sup>10, 11</sup> and ionic  $\text{NH}_4^+$  bound to Brønsted acid sites (1440  $\text{cm}^{-1}$ )<sup>8</sup> were observed clearly. Switching the feed gas to  $\text{NO} + \text{O}_2$  resulted in the decreases of both adsorbed  $\text{NH}_3$  and ionic  $\text{NH}_4^+$  peak intensities, indicating that both the coordinated  $\text{NH}_3$  and  $\text{NH}_4^+$  participated in the reduction of  $\text{NO}_x$ .

## References

- 1 B. Thirupathi and P.G. Smirniotis, *Appl. Catal. B*, 2011, **110**, 195-206.
- 2 E. B. Fox, S. Velua, M. H. Engelhard, Y. Chin, J. T. Miller, J. Kropf and C. Song, *J. Catal.*, 2008, **260**, 358-370.
- 3 G. Avrouropoulos and T. Ioannides, *Appl. Catal. A*, 2003, **244**, 155-167.
- 4 D. Yang, L. Wang, Y. Sun and K. Zhou, *J. Phys. Chem. C*, 2010, **114**, 8926-8932.
- 5 G. Qi, R. T. Yang and R. Chang, *Appl. Catal. B*, 2004, **51**, 93-106.
- 6 K.I. Hadjiivanov, *Catal. Rev. Sci. Eng.*, 2000, **42**, 71-144.
- 7 W. Shan, F. Liu, H. He, X. Shi and C. Zhang, *Chem. Commun.*, 2011, **47**, 8046-8048.
- 8 D.A. Peña, B.S. Uphade, E.P. Reddy and P.G. Smirniotis, *J. Phys. Chem. B*,

2004, **108**, 9927-9936.

9 W. Shan, F. Liu, H. He, X. Shi and C. Zhang, *Appl. Catal. B*, 2012, **115/116**,  
100-106.

10 G. Zhou, B. Zhong, W. Wang, X. Guan, B. Huang, D. Ye and H. Wu, *Catal.*  
*Today*, 2011, **175**, 157-163.

11 F. Liu, H. He, Y. Ding and C. Zhang, *Appl. Catal. B*, 2009, **93**, 194-204.

12 N.Y. Topsøe, *Science*, 1994, **265**, 1217-1219.